




## ORIGINAL ARTICLE OPEN ACCESS

# Investigating the Mechanism of IFN- $\gamma$ -Inducible Lysosomal Thiol Reductase-Mediated Inhibition of Breast Cancer Cell Proliferation

Qin Liu<sup>1</sup>  | Xiaoning Yuan<sup>1</sup> | Youcheng Shao<sup>1</sup> | Xiaoqing Guan<sup>1</sup> | Kaixiang Feng<sup>2</sup>  | Mengfei Chu<sup>3</sup> | Le Chen<sup>1</sup> | Hui Li<sup>1</sup> | Hanhui Liu<sup>1</sup> | Jingwei Zhang<sup>2</sup>  | Yihao Tian<sup>3</sup> | Lei Wei<sup>1</sup>

<sup>1</sup>Department of Pathology and Pathophysiology, Hubei Provincial Key Laboratory of Developmentally Originated Disease, TaiKang Medical School (School of Basic Medical Sciences), Wuhan University, Wuhan, Hubei, China | <sup>2</sup>Department of Breast and Thyroid Surgery, Zhongnan Hospital of Wuhan University, Hubei Key Laboratory of Tumor Biological Behaviors, Hubei Cancer Clinical Study Center, Wuhan, Hubei, China | <sup>3</sup>Department of Human Anatomy, TaiKang Medical School (School of Basic Medical Sciences), Wuhan University, Wuhan, Hubei, China

**Correspondence:** Lei Wei ([leiwei@whu.edu.cn](mailto:leiwei@whu.edu.cn)) | Jingwei Zhang ([zjwzhang68@whu.edu.cn](mailto:zjwzhang68@whu.edu.cn))

**Received:** 10 March 2024 | **Revised:** 27 August 2024 | **Accepted:** 18 September 2024

**Funding:** Fundamental Research Funds for the Central Universities (Grant No: 2042022FK1209); National Natural Science Funds of China (Grant No: 81972833); Basic and Clinical Medical Research Joint Fund of Zhongnan Hospital of Wuhan University (Grant No: JCZN2022008).

**Keywords:** breast cancer | IFN- $\gamma$ -inducible lysosomal thiol reductase | MYC | OICR-9429 | WDR5

## ABSTRACT

**Background:** Breast cancer has become a severe threat to human health, making it imperative to identify effective drugs and therapeutic targets.

**Methods:** Various molecular biology experiments, such as western blot analysis, cytologic effect, co-immunoprecipitation, and immunofluorescence assays, as well as a nude mouse xenograft tumor model, were used to comprehensively analyze the impact of gamma-interferon-inducible lysosomal thiol reductase (GILT) on the malignant phenotype of breast cancer cells. This work was performed to examine GILT expression levels and explore the potential mechanism in breast cancer.

**Results:** GILT protein expression levels were significantly lower in breast cancer cells than in normal breast epithelial cells. Over-expressing GILT inhibited breast cancer cell proliferation and migration and slowed tumor growth. GILT inhibited the interaction between the MYC and WDR5 transcription complex and played a tumor-suppressive role. The MYC/WDR5 transcription complex inhibitor OICR-9429 could synergize with GILT to inhibit breast cancer cell proliferation.

**Conclusion:** This study reveals a potential mechanism by which GILT can slow breast cancer growth, as well as identifying the possible clinical application value of small molecule inhibitor OICR-9429. These data collectively provide novel treatment strategies for breast cancer therapy.

## 1 | Introduction

Breast cancer is one of the most common malignant tumor types in women [1], with a high incidence that has become a severe public

health threat worldwide [2] and sadly affects many families. Because of the highly heterogeneous nature of breast cancer, identifying potential therapeutic targets is critical for guiding precision therapy approaches. With technological advancements and

**Abbreviations:** Co-IP, co-immunoprecipitation; GILT, IFN- $\gamma$ -inducible lysosomal thiol reductase; IC50, half-maximal inhibitory concentration; IFI30, interferon gamma-inducible protein 30; PI, propidium iodide.

Qin Liu, Xiaoning Yuan and Youcheng Shao contributed equally to this study and share the co-first authorship.

This is an open access article under the terms of the [Creative Commons Attribution-NonCommercial-NoDerivs](https://creativecommons.org/licenses/by-nc-nd/4.0/) License, which permits use and distribution in any medium, provided the original work is properly cited, the use is non-commercial and no modifications or adaptations are made.

© 2025 The Author(s). *Cancer Innovation* published by John Wiley & Sons Ltd on behalf of Tsinghua University Press.

the development of new diagnostic and therapeutic methods, breast cancer mortality rates are now on a downward trend [3]. Therefore, it is crucial to continue to find effective treatment strategies for breast cancer.

Interferon gamma-inducible protein 30 (IFI30), also called IFN- $\gamma$ -inducible lysosomal thiol reductase (GILT), is an enzyme localized to the endosome, lysosome, and phagosome [4] that catalyzes the reduction of disulfide bonds [5]. Studies have shown that GILT is involved in both tumor formation and cancer suppression but has an indispensable role in tumor progression. Data from Buetow et al. [6] suggest that GILT overexpression can improve melanoma patient survival rates, while Phipps-Yonas et al. [7] indicate that low GILT expression levels are associated with reduced B cell lymphoma patients survival. Similarly, other studies have shown that GILT plays a pro-cancer role in tumor development. In acute myeloid leukemia, Niu et al. [8] suggest that high GILT expression patterns are related to poor patient recovery, while low GILT expression levels can promote reactive oxygen species-mediated mitochondrial injury and apoptosis. In brain glioma, increased GILT expression is positively correlated with disease progression. Results from Chen et al. [9] suggest that low GILT expression levels can inhibit cell proliferation, migration, and tumor formation. However, the molecular mechanism of how GILT is involved in breast cancer remains unclear, leading us to explore this further in the current study.

MYC has been reported to be a driver gene of various malignancies [10]. C-Myc, an essential transcription factor, crucially contributes to cell proliferation, invasion, and apoptosis rates in different tumor types [11]. GILT is localized to the endosome and/or lysosome of cells and is closely related to autophagy. In addition, MYC can enhance LC-3II protein expression, inhibit P62 protein expression and autophagosome formation, and activate autophagy [12]. Therefore, we aimed to investigate the relationship between GILT and MYC.

As shown in our previous studies, targeting the MYC/WDR5 transcription complex is a potential therapeutic strategy for breast cancer because of the interaction between MYC and WDR5 in breast cancer cells. Because the carcinogenic properties of the MYC protein are closely related to its interaction with WDR5 [13], blocking this interaction may be a viable approach for targeting MYC [14]. MYC lacks small molecule-specific active sites and is mainly localized to the nucleus, making it a difficult molecular target. Therefore, we aimed to target WDR5. OICR-9429, a small molecule inhibitor of the MYC/WDR5 transcription complex, targets MYC/WDR5 and competitively binds to WDR5. This can thereby prevent the binding of the MYC/WDR5 transcription complex, which inhibits the cancer-promoting effects of MYC.

In this study, we examined the GILT protein expression levels, cytological effects, and protein interactions in breast cancer cells, as well as the pharmacological actions of OICR-9429. We speculated that the high expression levels of GILT in breast cancer cells would inhibit their proliferation and migration rates. OICR-9429 treatment inhibited the interaction between MYC and WDR5 in the transcription complex. Additionally, OICR-9429 could cooperate with GILT to exert anticancer effects and inhibit the MYC/WDR5 transcription complex. Therefore, our data indicate that GILT may be a latent therapeutic target for breast cancer, with the small

molecule inhibitor OICR-9429 also demonstrating potential clinical application.

## 2 | Materials and Methods

### 2.1 | Cell Culture

Experiments were conducted with the human mammary epithelial cell line MCF-10A, human breast cancer cell lines MCF-7 and MDA-MB-231, and HEK-293T cell line. Cells were cultured in high-glucose Dulbecco's Modified Eagle Medium containing 1% penicillin-streptomycin bis-antibody and 10% fetal bovine serum (FBS; Bio-Channel) in a controlled cell incubator at 5% CO<sub>2</sub>, 37°C, and saturated humidity.

### 2.2 | Plasmid Construction and Stable Cell Line Development

According to the target gene sequence, specific primers were designed using software and cloned into appropriate carrier plasmids. The plasmids were connected with T4 ligase (Servicebio) and used to transform bacteria. Then, clonal screening and identification were conducted to select the clones containing the correct insertion of the target gene.

shGILT-1:5'-GCGTTAGACTTCTTTGGAAT-3' (Human)

shGILT-2:5'-CCAGACACTATCATGGAGTGT-3' (Human)

shGILT-1:5'-GCTGGAGTGTAGACTGAACAT-3' (Mouse)

shGILT-2:5'-AGTAAAGGCATAACCTCAAAC-3' (Mouse)

The stable expression cell line was constructed and selected using the regular transformation method. Then, the identified positive plasmids, auxiliary packaging vector, and transfection reagent ZLip2000 (ZOMANBIO) were combined to transfect HEK-293T cells. The viral supernatants were collected after 48–72 h. The target cells were infected 6–8 h later, then cultured in complete medium for 48 h. The cells were selected using complete medium containing puromycin for 2 weeks. Finally, the protein and mRNA levels of target genes were examined to verify successful stable cell line construction.

### 2.3 | CCK-8 Assay

Cells in the logarithmic growth phase were seeded in 96-well plates at a density of  $3 \times 10^3$  cells/well. During the assay, 90  $\mu$ L of medium containing 10% FBS and 10  $\mu$ L CCK-8 solution (APExBIO) were added to each well and placed in the cell incubator for 2 h. Absorbance values at 450 nm were then measured using an enzyme labeler.

### 2.4 | Transwell Assay

Here,  $1 \times 10^4$  cells were seeded into a Transwell chamber and 10% FBS nutrient solution was added to 24-well plates. After cell

adhesion, the media in the upper and lower chambers were replaced with serum-free medium. The cells were then placed in the incubator overnight. The next day, the medium in the lower chamber was replaced with 20% FBS nutrient solution, while serum-free medium was kept in the upper chamber. The 24-well plates were placed in the incubator for 12–16 h, then the cells were fixed, stained, and counted.

## 2.5 | Colony Formation Assay

Here,  $1 \times 10^3$  cells were seeded into a 6-well plate and cultured in an incubator for about 2 weeks. The medium was changed every 2–3 days. The experiment was terminated after visible clones appeared on the plate. The cell colonies were fixed with paraformaldehyde, stained with crystal violet, and washed and dried. The stained cells were then observed and counted.

## 2.6 | Wound Healing Assay

Cells were seeded into a 6-well plate at a density of  $5 \times 10^5$  cells/well. After the cells reached approximately 80% confluency, a 10  $\mu$ L pipettor was used to create a scratch across each well. The medium was then removed and the cells were washed three times with sterile phosphate buffer saline. The medium was replaced with fresh serum-free or low-serum (< 2% FBS) medium and the cells were cultured in an incubator. At 0-, 24-, and 48-h timepoints, the cells were removed and the scratches were observed under a microscope and photographed.

## 2.7 | Flow Cytometry Analysis

For cell cycle detection,  $5 \times 10^5$  cells were collected in each tube, fixed with 70% ethanol, and placed at 4°C overnight. Propidium iodide (PI) was added, then red fluorescence was measured at 488 nm. FlowJo software was used for analysis.

For detecting apoptosis, the cells were induced according to the experimental protocol. Approximately  $1-5 \times 10^5$  cells and Annexin V-FITC and PI were added according to the apoptosis detection kit instructions. FlowJo software was used for analysis.

## 2.8 | Western Blot Analysis

Total protein was extracted from samples and quantified using the BCA protein assay kit. Electrophoresis was performed and the proteins were transferred to a membrane. The membrane was blocked with 5% skim milk and then incubated with the corresponding primary antibody overnight at 4°C. The next day, the membrane was incubated with the corresponding anti-rabbit or anti-mouse secondary antibody (1:10,000) at room temperature. Protein bands were detected using ECL reagent (Biosharp) and a computer-aided imaging analysis system (Tanon). GraphPad Prism Protein was used to analyze the bands. The primary antibodies used in this study were anti-GILT (Proteintech), anti-c-MYC (Proteintech), and anti-WDR5 (HUABIO).

## 2.9 | Nucleoplasmic Separation

For every 20  $\mu$ L of cell precipitation, 200  $\mu$ L of cytoplasmic protein extraction reagent A with PMSF was added, which dissolved in an ice bath after vortexing. Then, 10  $\mu$ L of cytoplasmic protein extraction reagent B was added, and the samples were vortexed and centrifuged. The resulting supernatants contained the extracted cytoplasmic proteins. For precipitation, 50  $\mu$ L of nuclear protein extraction reagent containing PMSF was added. For 30 min, the samples were vortexed every 1–2 min for 15–30 s and then placed back in the ice bath. After centrifugation, the resulting supernatants contained the extracted nuclear proteins.

## 2.10 | RNA Extraction and qPCR Analysis

For total RNA extraction, Trizol reagent was used to lyse the samples. Then, chloroform was added and the samples were centrifuged. Next, isopropyl alcohol was added for precipitation, followed by centrifugation, alcohol washing, and additional centrifugation. Finally, electrophoresis was used to examine RNA purity and a NanoDrop instrument was used to measure the RNA concentration.

Total RNA samples were reverse-transcribed into cDNA, which were then diluted according to the commonly used qPCR procedures. SYBR GREEN (Vazyme), primers, and RNase-free water were used to run qPCR analysis on a PCR instrument.

## 2.11 | Co-immunoprecipitation (Co-IP) Assay

This trial was roughly summarized as splitting the protein to obtain a mixture of proteins. The target protein antibody was mixed with the protein supernatant, then the complex was fixed and precipitated using antibody-conjugated beads. Elution was used to remove any proteins nonspecifically bound to the target protein. Finally, the pulled-down protein was detected using western blot analysis.

## 2.12 | Immunofluorescence

Cells were inoculated in a petri dish pre-placed with crawling tablets. The next day, the cells were fixed with 4% paraformaldehyde, permeated with 0.5% Triton X-100, and blocked with goat serum at room temperature. The samples were incubated with the primary antibody at 4°C for 12–16 h and then incubated with the fluorescently labeled secondary antibody at 37°C in the dark. DAPI was then added to stain the nuclei. The tablet was incubated with a sealing solution containing the anti-fluorescent quencher. Images were acquired using a fluorescence microscope.

## 2.13 | Mouse Xenograft Tumor Model

A 4T1 stable cell line was generated, then  $3 \times 10^6$  cells/150  $\mu$ L were subcutaneously inoculated into the armpits of BALB/c-nu nude mice (aged 4–6 weeks). Tumor growth was monitored for

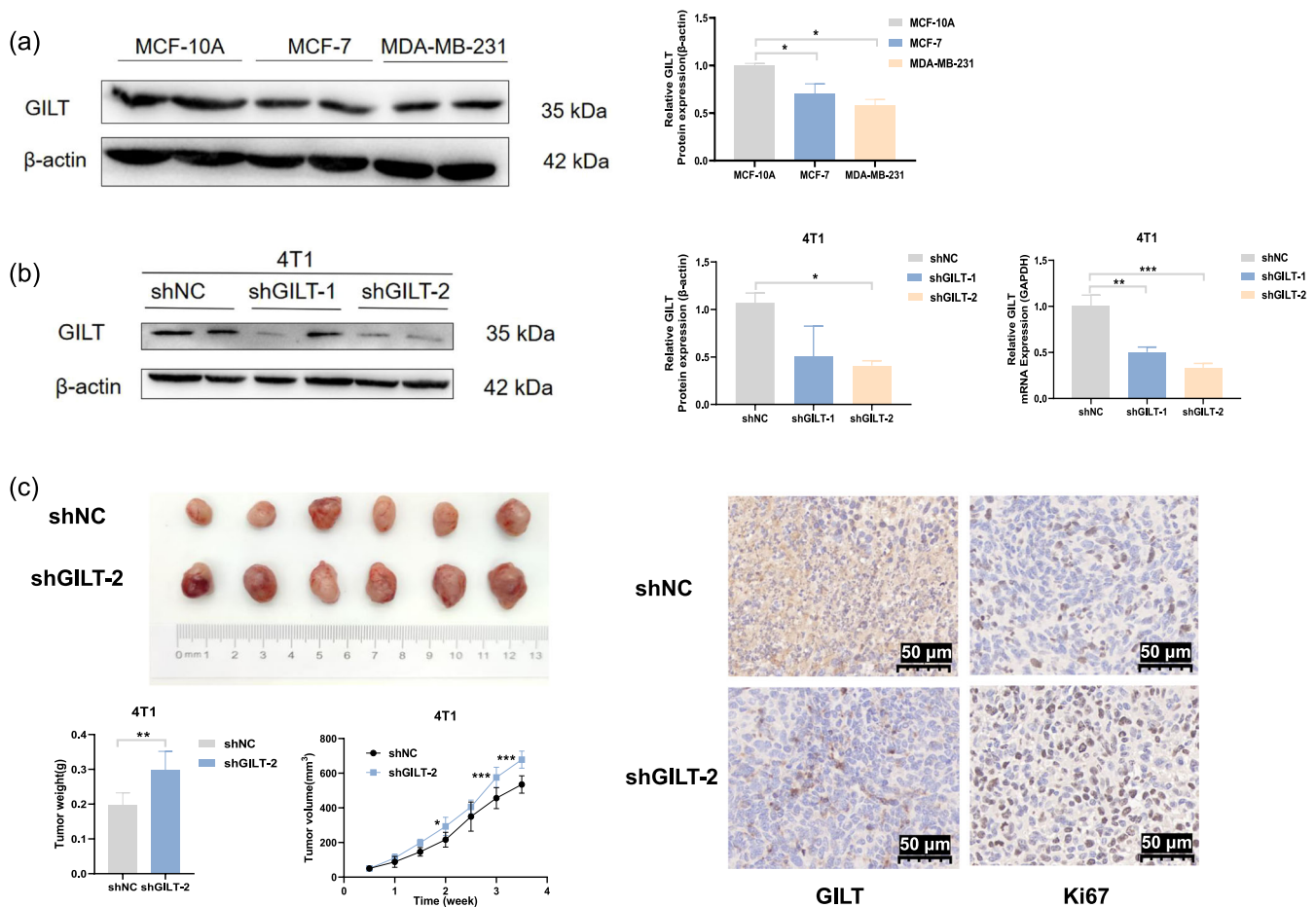


**FIGURE 1 |** GILT inhibits breast cancer cell proliferation. (a) GILT protein expression patterns in MCF-7 and MDA-MB-231 breast cancer cells and MCF-10A normal breast epithelial cells, as detected using western blot analysis. (b) Successful GILT knockdown was determined using western blot and qPCR analyses. (c) The effects of GILT knockdown on tumor growth were analyzed in a subcutaneous xenograft nude mice model. Immunohistochemistry (IHC) assays were used to examine Ki67 protein expression patterns. (\* $p < 0.05$ , \*\* $p < 0.01$ , \*\*\* $p < 0.001$ ).

1–2 weeks. After the mice were killed, the tumors were photographed, weighed, measured, and fixed with 4% paraformaldehyde. Immunofluorescence or immunohistochemistry (IHC) analysis was then performed on the tumor samples.

## 2.14 | Statistical Analysis

GraphPad Prism 7 software was used for statistical analysis. Each experiment was repeated three times, with data expressed as the mean  $\pm$  standard deviation. Differences between the two groups were compared using  $t$ -tests. All tests were two-tailed and a  $p < 0.05$  was considered statistically significant.

## 3 | Results

### 3.1 | GILT Inhibits Breast Cancer Cell Proliferation

We first detected GILT protein expression levels in breast epithelial cells and breast cancer cells. Compared with MCF-10A cells, GILT protein expression levels were significantly decreased in MCF-7 and MDA-MB-231 breast cancer cells (Figure 1a).

We then investigated the effects of GILT expression on tumor formation in xenograft models. 4T1 cells with GILT expression knocked down or control 4T1 cells (Figure 1b) were subcutaneously injected into the armpits of BALB/c nude mice. Compared with the control group, tumor growth rates were significantly higher in the GILT knockdown group. IHC assays demonstrated upregulated Ki67 protein levels in mouse tumors with GILT knockdown compared with the control group, indicating increased cell proliferation with lower GILT expression (Figure 1c).

These results suggest that GILT expression patterns are associated with breast cancer cell proliferation, with GILT inhibiting breast cancer growth.

### 3.2 | GILT Inhibits Breast Cancer Cell Proliferation and Migration, Inhibits Cell Cycle Progression, and Promotes Apoptosis

To explore the biological functions of GILT in breast epithelial cells, we constructed GILT knockdown or GILT overexpression stable cell lines. Successful generation of these cell lines was confirmed by western blot analysis (Figure 2a).

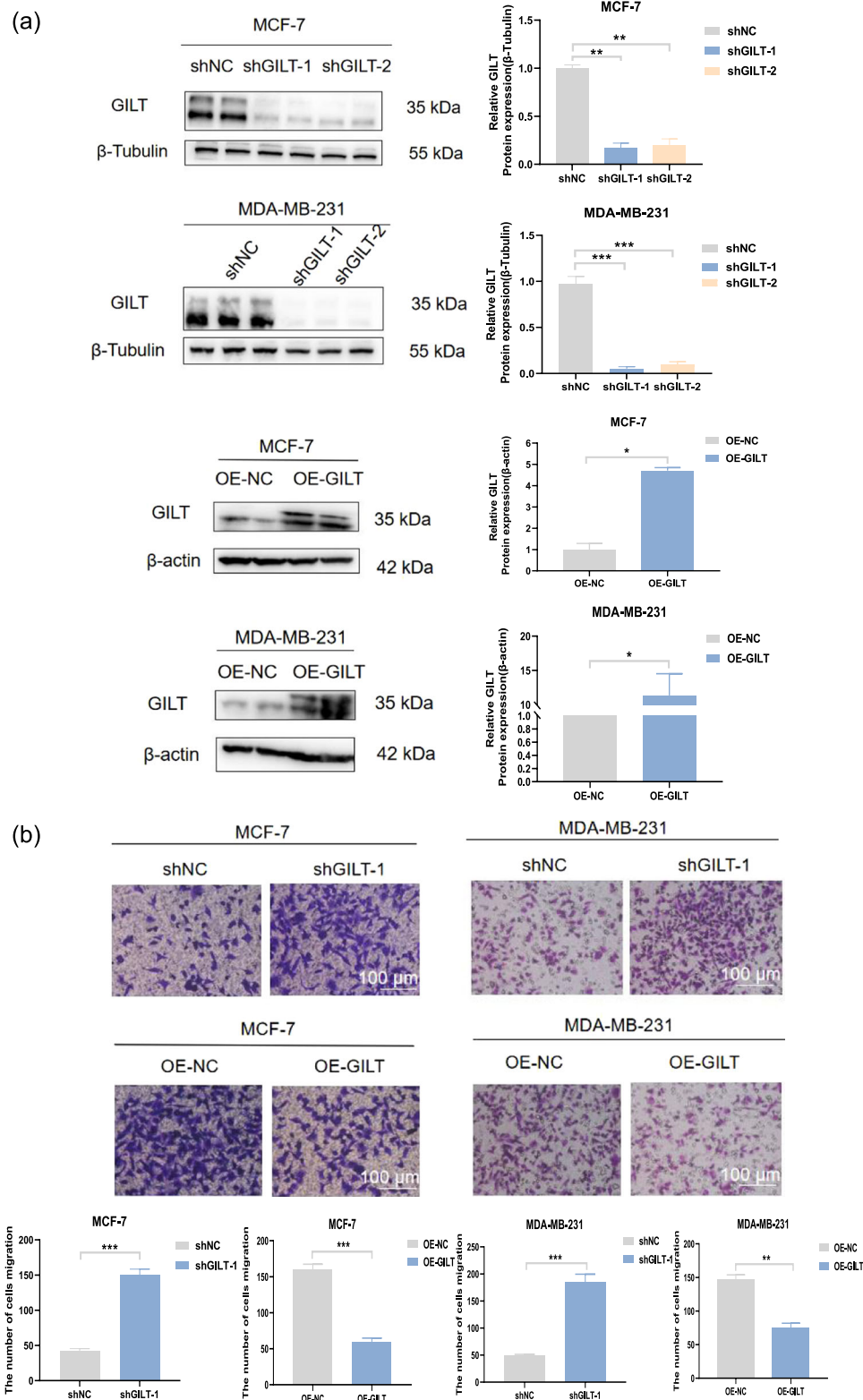


**FIGURE 2 |** GILT inhibits cell proliferation and migration, slows cell cycle progression, and promotes apoptosis in breast cancer cells. (a) Western blot analysis was used to validate stable cell line generation. (b) Transwell assays were used to detect the effects of GILT knockdown or overexpression on breast cancer cell migration rates. (c) The effects of GILT knockdown or overexpression on breast cancer cell proliferation were detected using CCK-8 assays. (d-e) Flow cytometry was used to examine breast cancer cell cycle progression and apoptosis levels. (\* $p < 0.05$ , \*\* $p < 0.01$ , \*\*\* $p < 0.001$ ).



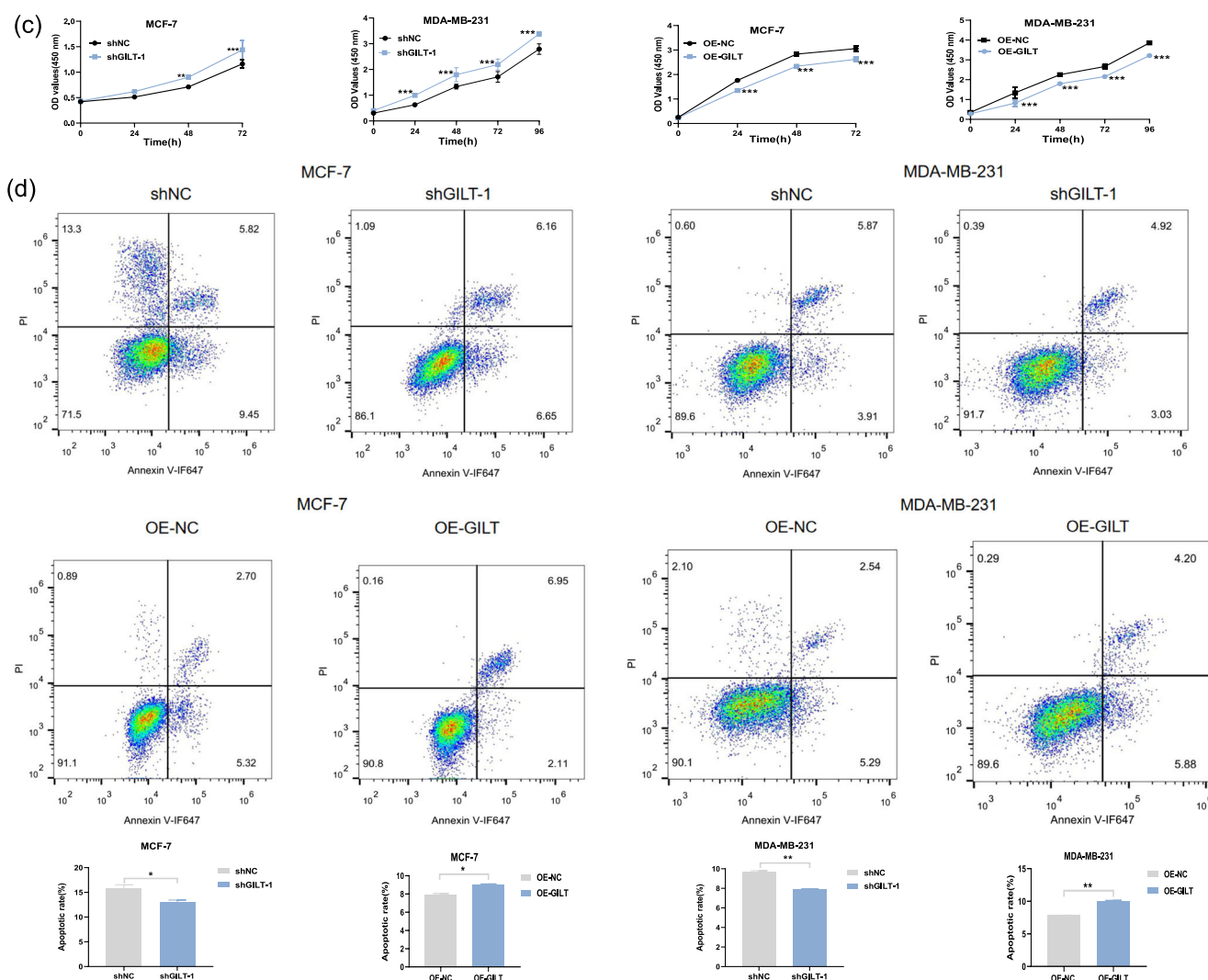


**FIGURE 2 |** (Continued)

Transwell experiments were performed to investigate the effects of GILT expression on breast cancer cell motility. Compared with the control group, GILT knockdown promoted breast cancer cell migration, while overexpressing GILT inhibited breast cancer cell migration (Figure 2b). We also performed CCK-8 assays to investigate how GILT expression impacted breast cancer cell proliferation. When GILT was knocked down in breast cancer cells, the cell proliferation rate significantly increased compared with that of the control group. Conversely, GILT overexpression significantly reduced the breast cancer cell proliferation rate (Figure 2c).

Next, we evaluated the effects of GILT expression on breast cancer cell apoptosis and cell cycle progression using flow cytometry. Compared with the control group, GILT knockdown led to inhibited early and late apoptosis levels, a reduced proportion of cells in the G1/G0 phase, and an increased ratio of cells in the S + G2/M phase. Overexpression of GILT had the opposite effects, with increased breast cancer cell early and late apoptosis levels, a higher

proportion of cells in the G1/G0 phase, and fewer cells in the S + G2/M phase (Figure 2d,e).

These results suggest that GILT may act as a tumor suppressor gene by inhibiting breast cancer cell growth and migration.

### 3.3 | GILT Inhibits the Interaction Between the MYC/WDR5 Transcription Complex

MYC amplification and migration are closely related to tumorigenesis (Supporting Information S1: Figure S1a–e) and cancer patient outcomes. Immunofluorescence analysis of tissue specimens showed colocalization between the GILT and MYC proteins (Figure 3a). Additionally, interactions between the GILT and MYC proteins in breast cancer cells were detected using co-IP experiments (Figure 3b). After GILT overexpression in MCF-7 and MDA-MB-231 breast cancer cells, a MYC plasmid was also transfected to overexpress MYC. CCK-8 assay data showed that overexpressing MYC could reduce the ability of GILT to inhibit breast cancer cell proliferation (Figure 3c). Furthermore, the Transwell experimental

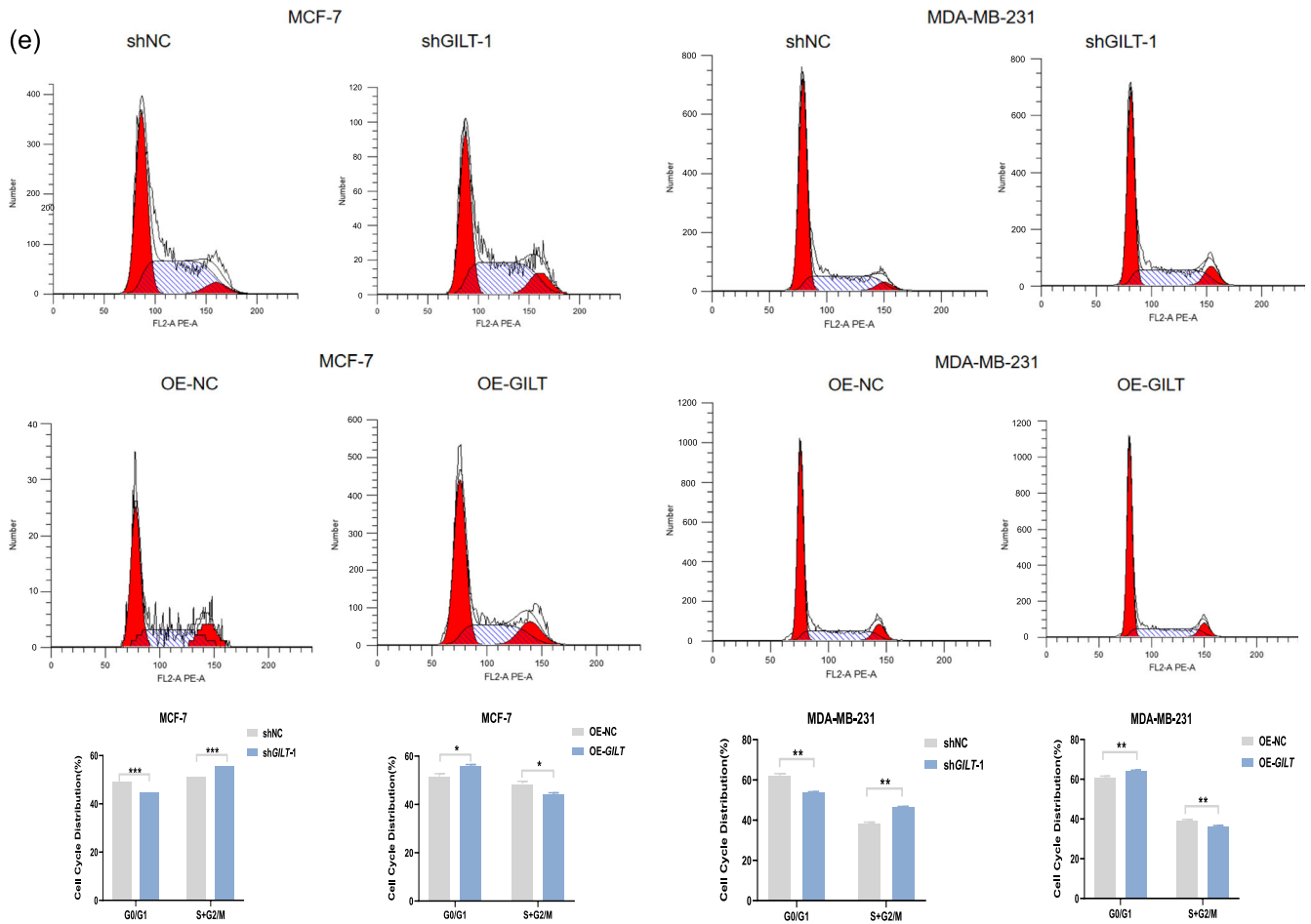


**FIGURE 2** | (Continued)

results showed that MYC overexpression could prevent GILT from inhibiting breast cancer cell migration (Figure 3d). Subsequently, we used co-IP experiments to demonstrate interactions between WDR5 and GILT and between WDR5 and MYC in these cells (Figure 3e).

Immunofluorescence assays showed that GILT was localized to the cytoplasm and nucleus (Figure 3f). Western blot analysis of the different protein fractions indicated that GILT was distributed in both the cytoplasm and nucleus, while MYC was primarily distributed in the nucleus (Figure 3g).

We then predicted the GILT entry signal peptide using cNLS Mapper (Figure 3h) to explore the corresponding anticancer effects of GILT. We constructed a FLAG-tagged GILT overexpression vector, as well as a GILT overexpression vector with the inbound signal peptide removed (Figure 3i). The immunofluorescence results showed that the GILT fluorescence intensity in the nucleus increased when the FLAG tag was successfully expressed and the incoming signal peptide was present. When the incoming signal peptide was removed, the GILT fluorescence in the nucleus decreased (Figure 3j). Moreover, the interaction between WDR5 and MYC was enhanced in stable cells with GILT knockdown compared with the control group. The interaction between these two proteins was weakened in breast

cancer cells with GILT overexpression compared with the control group (Figure 3k).

These experimental results suggest that GILT can inhibit the interaction between MYC and WDR5 after entering the nucleus from the cytoplasm, which contributes to its anticancer effects.

### 3.4 | OICR-9429, a Small Molecule Inhibitor of the MYC/WDR5 Transcription Complex, Synergizes With GILT to Exert Tumor-Suppressive Effects

Because of the lack of small molecule-specific active sites and its nuclear localization, MYC is difficult to therapeutically target. Previous studies have reported that MYC can interact with WDR5. Therefore, WDR5 was selected as the entry point, with the OICR-9429 molecule competitively binding to WDR5 to inhibit the cancer-promoting effects of MYC. Breast cancer cell proliferation rates following treatment with various OICR-9429 concentrations (0, 5, 10, 20, 40, and 80  $\mu$ M) were examined using CCK-8 assays. The data demonstrated that the half-maximal inhibitory concentration (IC<sub>50</sub>) of the drug was 40  $\mu$ M (Figure 4a). The effects of OICR-9429 on breast cancer cell proliferation were then detected by CCK-8 and clonal formation assays at the IC<sub>50</sub>. Compared with the control group, breast

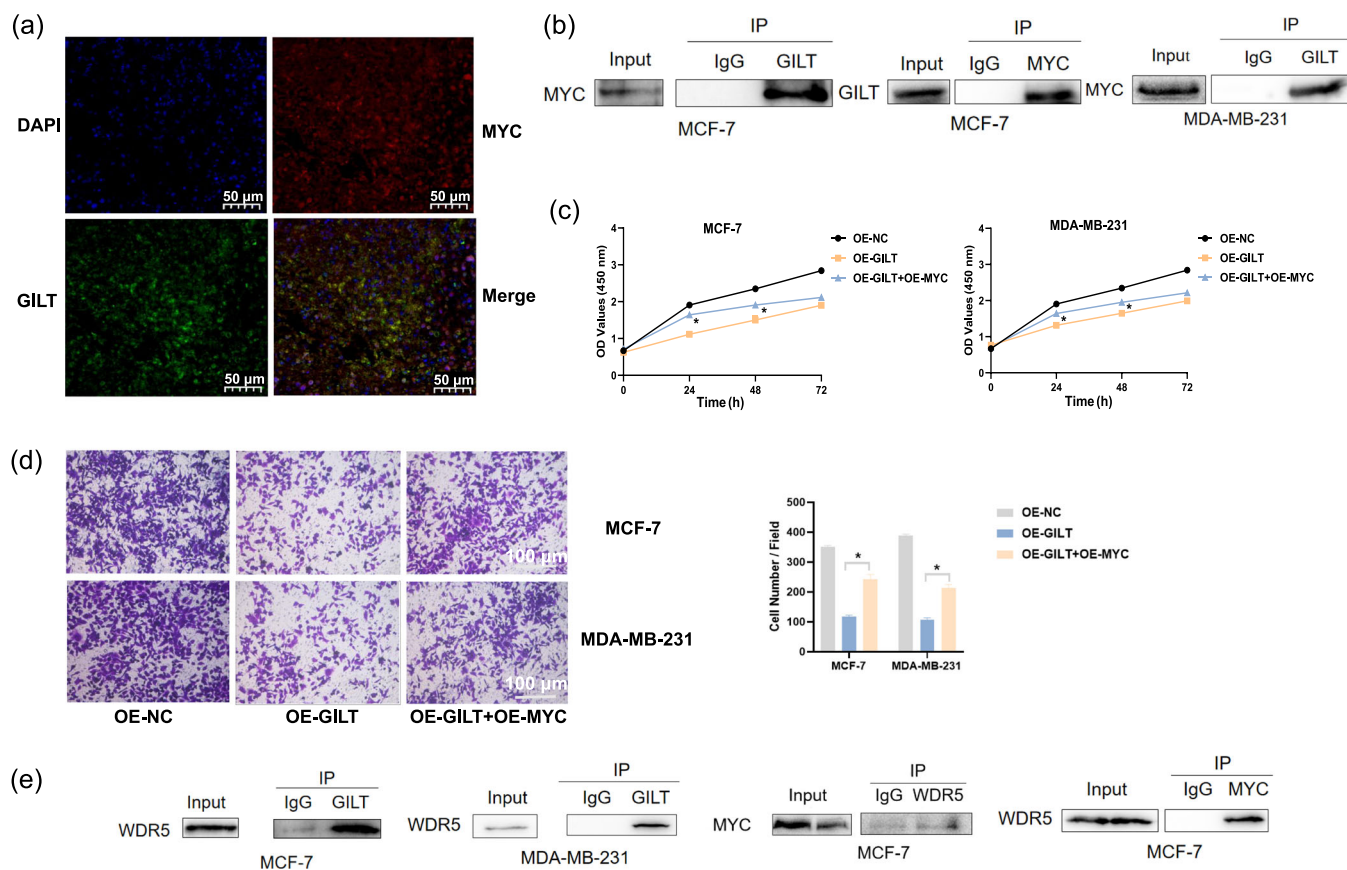


**FIGURE 3 |** GILT inhibits the interaction between the MYC/WDR5 transcription complex. (a, b) The interaction between GILT and MYC was detected using immunofluorescence assays and co-IP experiments. (c, d) CCK-8 and Transwell assays were used to detect the effects of MYC overexpression on the ability of GILT to inhibit breast cancer cell proliferation and migration. (e) The interactions between GILT, WDR5, and MYC were examined using co-IP experiments. (f) Immunofluorescence assays were used to detect the cellular localization of GILT. (g) Western blot analysis was used to detect the distribution of GILT and MYC proteins in the cytoplasm and nucleus. (h, i) cNLS Mapper was used to detect the GILT inbound signal peptide. Then, a FLAG-tagged GILT overexpression vector and GILT overexpression vector with the inbound signal peptide removed were constructed. Western blot analysis indicated the successful expression of the FLAG tag. (j) Immunofluorescence experiments with FLAG tags detected the effects of nucleus-entering signal peptides on GILT. (k) Co-immunoprecipitation experiments were used to detect the impact of GILT on the MYC/WDR5 transcription complex. (\* $p < 0.05$ , \*\* $p < 0.01$ , \*\*\* $p < 0.001$ ).

cancer cell proliferation was inhibited following OICR-9429 treatment (Figure 4b). Transwell experiments were used to examine how OICR-9429 can affect breast cancer cell migration at the IC50, which indicated lower migration rates following OICR-9429 treatment (Figure 4c).

OICR-9429 is particularly important in targeting the c-MYC interacting protein complex. We therefore used co-IP experiments to detect changes in the MYC and WDR5 interaction before and after treatment. Compared with the control group, the interaction between MYC and WDR5 was inhibited after OICR-9429 was added (Figure 4d).

We further studied the effect of OICR-9429 treatment on tumor formation in xenograft models. 4T1 cells with GILT knockdown and control 4T1 cells were subcutaneously injected into the armpit of BALB/c nude mice. After tumor formation a week later, DMSO was added to the control group and OICR-9429 was added to the treatment group. The results showed that OICR-9429 treatment significantly reduced tumor growth compared with the control group, with IHC staining of mouse tumors indicating

downregulated Ki67 protein expression levels with OICR-9429 treatment (Figure 4e). In breast cancer cells overexpressing GILT, experiments using the EdU method showed that OICR-9429 synergized with GILT to significantly inhibit breast cancer cell proliferation compared with the control group (Figure 4f).

Collectively, these in vivo and in vitro experimental results suggest that the small molecule inhibitor OICR-9429 can synergize with GILT to exert tumor-suppressive effects, providing a novel therapeutic strategy for effectively treating breast cancer.

## 4 | Discussion

Breast cancer can occur in women of all ages. The incidence of this disease is continuously increasing, ranking first among female malignant tumor types in China. Therefore, research into new treatment methods for breast cancer has been ongoing. Therapeutic approaches include initial local surgical treatment and various systemic treatment methods, such as



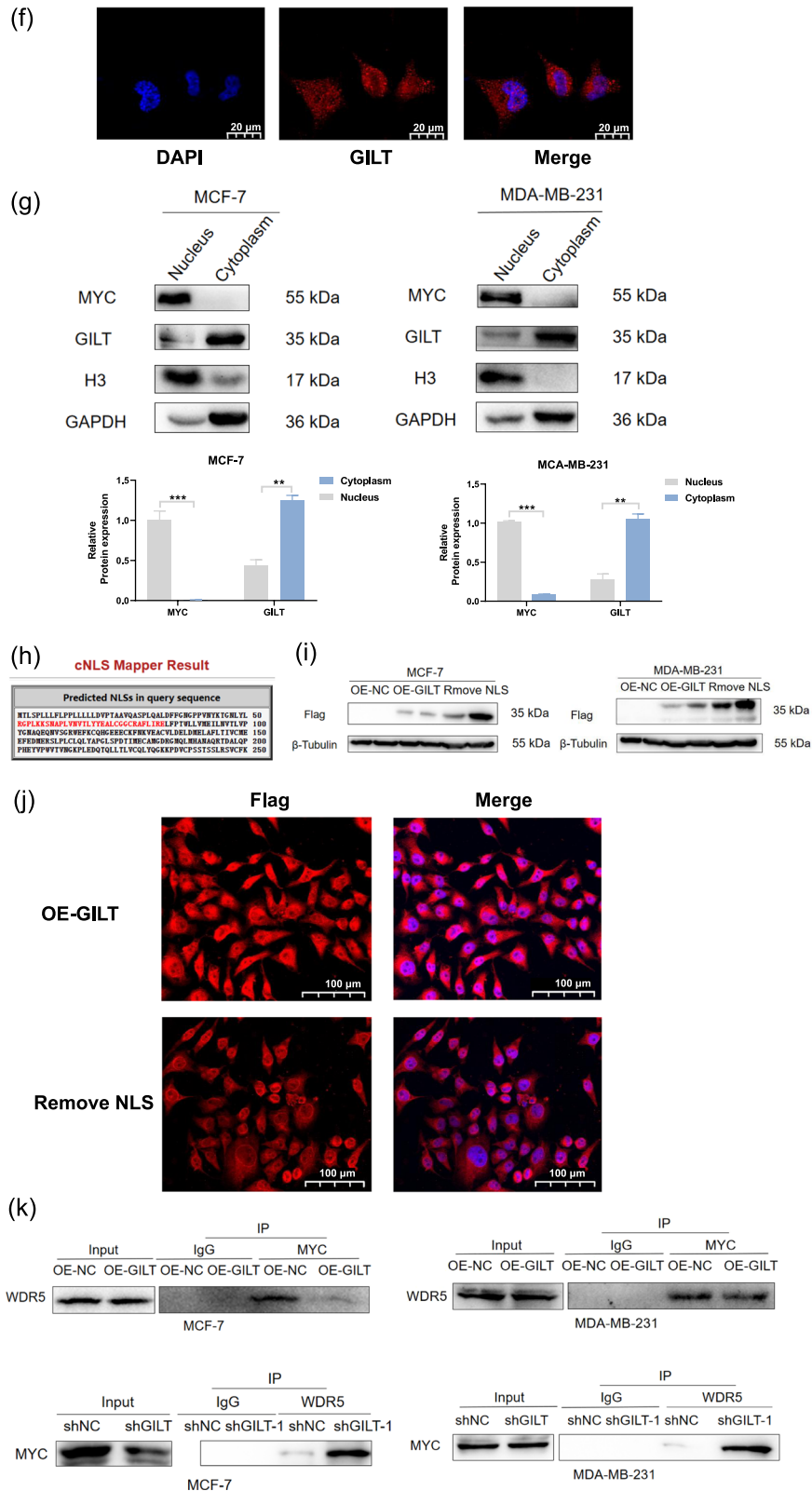


**FIGURE 3** | (Continued)

hormone therapy, adjuvant chemotherapy, and biological therapy. The current research trend is exploring targeted therapy strategies to identify specific molecular targets that can effectively target cancer cells and minimally affect the surrounding normal cells.

GILT is expressed in most antigen-presenting cells [15], such as monocytes/macrophages, B cells, and bone marrow dendritic cells [16]. GILT expression can be induced by interferon- $\gamma$  in other cell types [17], such as fibroblasts, epidermal cells, and keratinocytes [18]. GILT is also differentially expressed between breast cancer

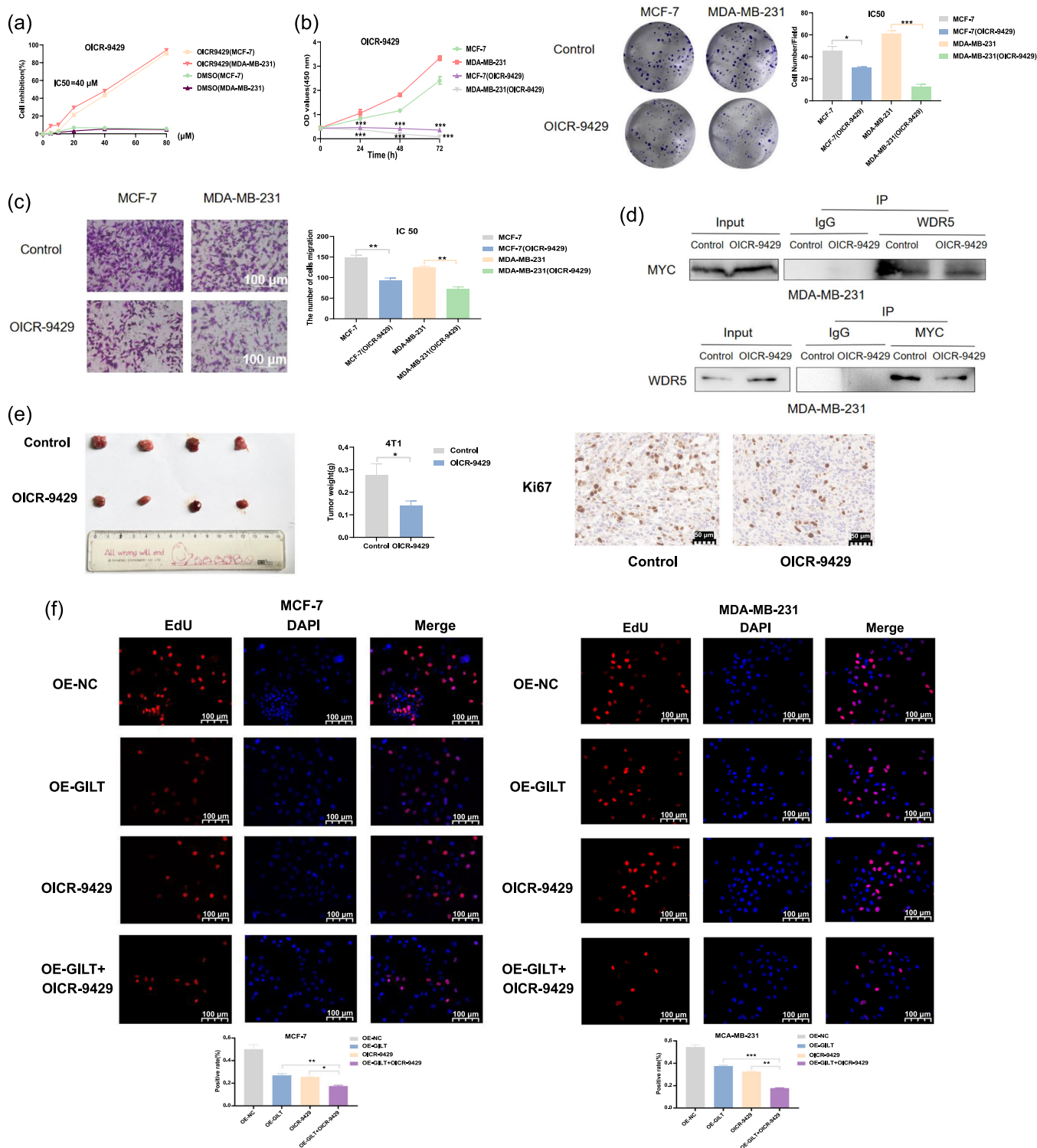


**FIGURE 4 |** OICR-9429 synergizes with GILT to exert tumor-suppressive effects. (a) CCK-8 assays were used to detect the half-maximal inhibitory concentration (IC50) of OICR-9429 in breast cancer cells. (b) The effects of OICR-9429 on breast cancer cell proliferation were detected using plate cloning and CCK-8 methods. (c) The effects of OICR-9429 on breast cancer cell migration were examined using the Transwell method. (d) The effects of OICR-9429 on the MYC/WDR5 transcription complex were detected using co-IP assays. (e) The effects of OICR-9429 on solid tumor growth were analyzed using a subcutaneous xenograft nude mouse model. (f) EdU assays were used to detect the effects of OICR-9429 synergizing with GILT on breast cancer cell proliferation. (\* $p < 0.05$ , \*\* $p < 0.01$ , \*\*\* $p < 0.001$ ).

tissues and adjacent normal tissues [19]. In this study, over-expressing GILT could inhibit breast cancer cell proliferation. The low expression levels of GILT observed in breast cancer cell lines suggest that GILT may be involved in tumor suppression in breast

tissues. To determine the function of GILT in breast cancer, we conducted various in vitro and in vivo experiments. The results showed that GILT could inhibit breast cancer cell proliferation and migration, as well as promote their apoptosis.

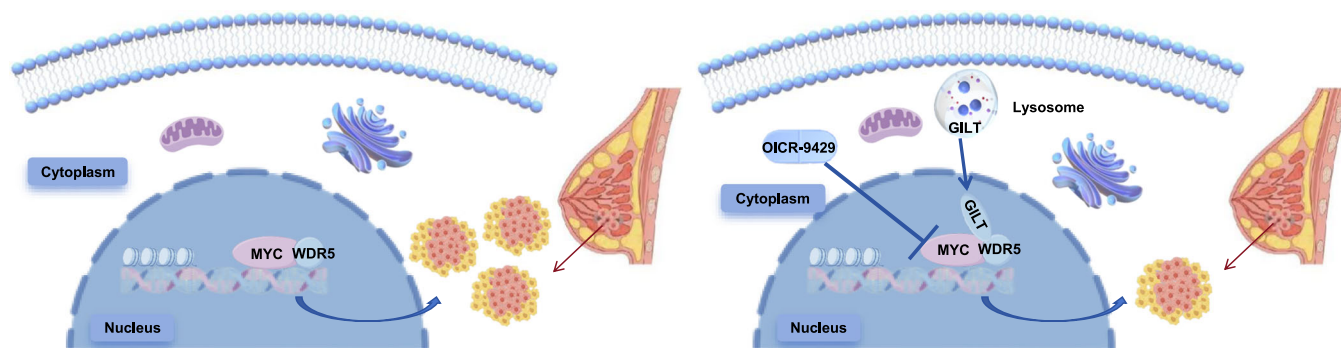


**FIGURE 5** | OICR-9429 synergizes with GILT to inhibit breast cancer cell proliferation.

In this study, the MYC and GILT proteins were found to interact, suggesting that they may be involved in a regulatory mechanism that can affect breast cancer progression. According to the previous experimental results of our research group, MYC and WDR5 can interact. Additionally, WDR5 can form a complex with certain proteins. This interaction between MYC and WDR5 can inhibit tumor growth [20]. Co-IP experiments were used to confirm this interaction in breast cancer cells. Following GILT knockdown, the MYC and WDR5 interaction was enhanced, while the opposite effects were observed after overexpressing GILT. These experiments indicated that GILT may inhibit the interaction between MYC and WDR5 by also interacting with these proteins after entering the nucleus, thus exerting tumor-suppressive effects.

MYC lacks small molecule-specific active sites and is mainly localized to the nucleus, making it difficult to target. Therefore, we selected WDR5 as the entry point and used the small molecule inhibitor OICR-9429 to competitively bind to WDR5, thereby inhibiting the interaction between the MYC/WDR5 transcription complex and blocking the cancer-promoting effects. At the molecular level, GILT can co-inhibit the MYC/WDR5 transcription complex to support anticancer effects. In this study, our data showed that OICR-9429 could synergize with GILT to inhibit breast cancer cell proliferation and migration. Co-IP results suggested that OICR-9429 treatment inhibited the interaction of the MYC/WDR5 transcription complex in breast cancer cells.

## 5 | Conclusion

In summary, the model depicted in Figure 5 shows that GILT can inhibit the interaction between the MYC/WDR5 transcription complex after entering the nucleus, exerting tumor suppressor effects. In addition, OICR-9429 can synergistically inhibit breast cancer cell proliferation and migration together with GILT. GILT is a potential therapeutic target and provides new options for breast cancer treatment. OICR-9429-mediated inhibition of the MYC/WDR5 transcription complex is of great significance for clinical applications, providing a novel strategy for improving poor prognosis in breast cancer patients.

### Author Contributions

**Qin Liu:** data curation (equal), writing – original draft (equal), writing – review and editing (equal). **Xiaoning Yuan:** conceptualization (equal).

**Youcheng Shao:** project administration (equal). **Xiaoqing Guan:** investigation (equal). **Kaixiang Feng:** formal analysis (equal). **Mengfei Chu:** data curation (equal). **Le Chen:** formal analysis (equal). **Hui Li:** formal analysis (equal). **Hanhui Liu:** writing – review and editing (equal). **Jingwei Zhang:** project administration (equal). **Yihao Tian:** project administration (equal). **Lei Wei:** project administration (equal).

### Acknowledgments

The authors have nothing to report.

### Ethics Statement

The authors have nothing to report.

### Consent

The authors have nothing to report.

### Conflicts of Interest

The authors declare no conflicts of interest.

### Data Availability Statement

The data presented in this study are available upon request from the corresponding author.

### References

1. J. Ferlay, I. Soerjomataram, R. Dikshit, et al., “Cancer Incidence and Mortality Worldwide: Sources, Methods and Major Patterns in GLOBOCAN 2012,” *International Journal of Cancer* 136, no. 5 (2015): E359–E386, <https://doi.org/10.1002/ijc.29210>.
2. R. L. Siegel, K. D. Miller, N. S. Wagle, and A. Jemal, “Cancer Statistics, 2023,” *CA: A Cancer Journal for Clinicians* 73, no. 1 (2023): 17–48, <https://doi.org/10.3322/caac.21763>.
3. E. Tarighati, H. Keivan, and H. Mahani, “A Review of Prognostic and Predictive Biomarkers in Breast Cancer,” *Clinical and Experimental Medicine* 23, no. 1 (2023): 1–16, <https://doi.org/10.1007/s10238-021-00781-1>.
4. K. Honey, M. Duff, C. Beers, et al., “Cathepsin S Regulates the Expression of Cathepsin L and the Turnover of  $\gamma$ -Interferon-Inducible Lysosomal Thiol Reductase in B Lymphocytes,” *Journal of Biological Chemistry* 276, no. 25 (2001): 22573–22578, <https://doi.org/10.1074/jbc.M101851200>.
5. M. P. Rausch and K. T. Hastings, “Diverse Cellular and Organismal Functions of the Lysosomal Thiol Reductase GILT,” *Molecular Immunology* 68, no. 2 Pt A (2015): 124–128, <https://doi.org/10.1016/j.molimm.2015.06.008>.
6. K. H. Buetow, L. R. Meador, H. Menon, et al., “High Gilt Expression and an Active and Intact MHC Class II Antigen

Presentation Pathway Are Associated With Improved Survival in Melanoma,” *Journal of Immunology* 203, no. 10 (2019): 2577–2587, <https://doi.org/10.4049/jimmunol.1900476>.

7. H. Phipps-Yonas, H. Cui, N. Sebastiao, et al., “Low GILT Expression Is Associated With Poor Patient Survival in Diffuse Large B-Cell Lymphoma,” *Frontiers in Immunology* 4 (2013): 425, <https://doi.org/10.3389/fimmu.2013.00425>.

8. L. T. Niu, Y. Q. Wang, C. C. L. Wong, S. X. Gao, X. D. Mo, and X. J. Huang, “Targeting IFN- $\gamma$ -Inducible Lysosomal Thiol Reductase Overcomes Chemoresistance in AML Through Regulating the Ros-Mediated Mitochondrial Damage,” *Translational Oncology* 14, no. 9 (2021): 101159, <https://doi.org/10.1016/j.tranon.2021.101159>.

9. S. Chen, Q. Wang, X. Shao, et al., “Lentivirus Mediated  $\gamma$ -Interferon-Inducible Lysosomal Thiol Reductase (GILT) Knockdown Suppresses Human Glioma U373MG Cell Proliferation,” *Biochemical and Biophysical Research Communications* 509, no. 1 (2019): 182–187, <https://doi.org/10.1016/j.bbrc.2018.12.099>.

10. C. V. Dang, “A Time for MYC: Metabolism and Therapy,” *Cold Spring Harbor Symposia on Quantitative Biology* 81 (2016): 79–83, <https://doi.org/10.1101/sqb.2016.81.031153>.

11. P. A. Carroll, B. W. Freie, H. Mathsyaraja, and R. N. Eisenman, “The MYC Transcription Factor Network: Balancing Metabolism, Proliferation and Oncogenesis,” *Frontiers of Medicine* 12, no. 4 (2018): 412–425, <https://doi.org/10.1007/s11684-018-0650-z>.

12. J. Zhu, M. Huang, P. Jiang, J. Wang, R. Zhu, and C. Liu, “Myclobutanil Induces Neurotoxicity by Activating Autophagy and Apoptosis in Zebrafish Larvae (*Danio rerio*),” *Chemosphere* 357 (2024): 142027, <https://doi.org/10.1016/j.chemosphere.2024.142027>.

13. E. Froimchuk, Y. Jang, and K. Ge, “Histone H3 Lysine 4 Methyltransferase KMT2D,” *Gene* 627 (2017): 337–342, <https://doi.org/10.1016/j.gene.2017.06.056>.

14. S. Chacón Simon, F. Wang, L. R. Thomas, et al., “Discovery of WD Repeat-Containing Protein 5 (WDR5)-MYC Inhibitors Using Fragment-Based Methods and Structure-Based Design,” *Journal of Medicinal Chemistry* 63, no. 8 (2020): 4315–4333, <https://doi.org/10.1021/acs.jmedchem.0c00224>.

15. M. Vedadi, L. Blazer, M. S. Eram, D. Barsyte-Lovejoy, C. H. Arrowsmith, and T. Hajian, “Targeting Human SET1/MLL Family of Proteins,” *Protein Science* 26 (2017): 662–676, <https://doi.org/10.1002/pro.3129>.

16. B. Arunachalam, U. T. Phan, H. J. Geuze, and P. Cresswell, “Enzymatic Reduction of Disulfide Bonds in Lysosomes: Characterization of a Gamma-Interferon-Inducible Lysosomal Thiol Reductase (GILT),” *Proceedings of the National Academy of Sciences USA* 97, no. 2 (2000): 745–750, <https://doi.org/10.1073/pnas.97.2.745>.

17. M. Maric, B. Arunachalam, U. T. Phan, et al., “Defective Antigen Processing in GILT-Free Mice,” *Science* 294, no. 5545 (2001): 1361–1365, <https://doi.org/10.1126/science.1065500>.

18. U. T. Phan, M. Maric, T. P. Dick, and P. Cresswell, “Multiple Species Express Thiol Oxidoreductases Related to GILT,” *Immunogenetics* 53, no. 4 (2001): 342–346, <https://doi.org/10.1007/s002510100323>.

19. M. P. Rausch, K. R. Irvine, P. A. Antony, N. P. Restifo, P. Cresswell, and K. T. Hastings, “GILT Accelerates Autoimmunity to the Melanoma Antigen Tyrosinase-Related Protein 1,” *Journal of Immunology* 185, no. 5 (2010): 2828–2835, <https://doi.org/10.4049/jimmunol.1000945>.

20. L. R. Thomas, C. M. Adams, J. Wang, et al., “Interaction of the Oncoprotein Transcription Factor MYC With Its Chromatin Cofactor WDR5 Is Essential for Tumor Maintenance,” *Proceedings of the National Academy of Sciences USA* 116, no. 50 (2019): 25260–25268, <https://doi.org/10.1073/pnas.1910391116>.

## Supporting Information

Additional supporting information can be found online in the Supporting Information section.